Research Article Vol. 56, No. 33 / November 20 2017 / Applied Optics 9225

applied optics

Absorption measurements in optical coatings by lock-in thermography

Feng Liu and Laurent Gallais*

Aix Marseille Univ, CNRS, Centrale Marseille, Institut Fresnel, UMR 7249, 13013 Marseille, France
*Corresponding author: laurent.gallais@fresnel.fr

Received 14 August 2017; revised 20 October 2017; accepted 23 October 2017; posted 23 October 2017 (Doc. ID 304714); published 14 November 2017

We evaluate and apply lock-in thermography as a method to quantitatively evaluate absorption losses of optical coatings. The principle of the method consists of applying periodically modulated laser intensity on the coatings and to monitor the periodic surface temperature evolution with an infrared camera. By application of a lock-in correlation procedure and using calibrated absorption samples, it is possible to obtain quantitative absorption values and to obtain absorption mappings with spatial resolution that depends on the optical configuration. Numerical simulations and experiments were performed in the case of 10–60 W laser irradiation at 1060 nm on different single layer coatings and highly reflective mirrors. In the tested conditions, the measurement of absorption down to 1 ppm level could be reached. The advantages, limitations, and potential applications of the technique are discussed.

OCIS codes: (310.6860) Thin films, optical properties; (350.5340) Photothermal effects.

https://doi.org/10.1364/AO.56.009225

1. INTRODUCTION

High-power lasers are used in numerous applications, and their power scaling breaks new records at a fast rate. This is particularly the case for fiber lasers that can reach multi-kW output powers with diffraction-limited beam quality [1]. Absorption in optical coatings is one of the main limitations of the power-handling capability of optical components for such laser systems. This absorption can be intrinsic to the deposited materials or localized due to the presence of defects related to the manufacturing process or environmental contamination. Indeed, different kinds of defects related to the manufacturing process (polishing residues, pits, scratches, coating impurities, nodules, etc.) or the operating environment (organic or particulate contamination) can lead to energy absorption. Absorption of laser radiation in the coating, heat diffusion, and subsequent increase of temperature in the optical component can be detrimental for the optics with consequences going from wavefront distortion to damage from thermomechanical stresses. Techniques for evaluation of absorption losses and measurements of power handling capacity of the components are therefore required for developments and optimizations of high-power laser optics.

The most widely used methods for absorption measurement are laser calorimetry [2] and techniques related to photothermal effects [3]. The calorimetry technique directly measures the absolute absorptance of the sample by using a temperature sensor to monitor the absorption-induced temperature rise inside the sample and then calibrating the absorbed energy with the incident radiation power. The limit for this method is that it needs relatively long irradiation time and cooling time to achieve reliable results [4]. Several methods applying different photothermal effects are also used for measuring the absorptance in optical components, such as photothermal deflection [5], photothermal displacement [6], photothermal detuning [7], and surface thermal lens effect [8]. Such techniques are sensitive and fast, and mapping of the absorption [9] can be achieved, but the measurement results need to be calibrated with optical, thermal, and thermoelastic properties of the investigated sample to finally evaluate the absorptance. Mühlig *et al.* [10] applied a laser-induced deflection technique for the measurement; in this technique, an electrical calibration procedure was needed. Some other works are carried out to aggregate multiple techniques to combine several advantages for measuring the absorptance, e.g., Li *et al.* [11] have combined the calorimetry and the photothermal technique, and Steinlechner *et al.* [12] have combined the photothermal self-phase-modulation and the cavity ring-down spectroscopy techniques, but the systems are more complex.

In this work, we investigate an alternative to such techniques by the use of infrared thermography (IRT) for direct monitoring of the temperature increase subsequent to high-power laser radiation absorption. The main motivation for this investigation is to develop a simple experiment to directly quantify the absorption level and detect absorption inhomogeneities

(defects) on full-scale optics (few centimeters). Indeed sensitive absorption measurement techniques, such as laser calorimetry or other photothermal techniques that were described previously, provide usually point measurements, and a displacement of the sample or the beam is required to obtain a 2D mapping. Direct infrared thermographic measurements, however, combined with laser illumination in the field of view of the IR camera, have the ability to provide direct 2D measurements. Such measurements can be possible and easily implemented based on the recent advances in fiber lasers that can provide the high power required to illuminate a full-scale optic and progress in the development of new and better infrared cameras. However, because the signal is expected to be very weak in the case of low absorption, we have applied lock-in thermography (LIT) techniques [13] to increase the signal-to-noise ratio. The LIT, also known as thermal wave imaging, is an active thermography technique that can be used to achieve enhanced signal-to-noise ratio. In this technique, the heat introduction occurs periodically with a certain lock-in frequency, and the local surface temperature modulation is evaluated and averaged over a number of periods, by evaluating only the oscillating part of the detected signal. In such conditions, the thermal drifts and the stray light from the surroundings can be effectively eliminated. By applying a quadrature correlation procedure, the thermal wave amplitude and the phase, which relate to the delay caused by the heat penetration depth, can be retrieved [14,15]. This technique had been used in non-destructive detection of subsurface defects in bulk materials [16,17], of thermal contact characterization [18], of biology and medicine [19,20], failure analysis of ICs [21], and testing on solar cell components. In this last field, e.g., it has been applied to the measurement of the carrier lifetime [22] and the carrier density [23], identifying the shunts [24] and monitoring the power loss [25,26].

The first part of the paper is dedicated to the description of this technique and theoretical considerations for application to optical coatings. Then, in the second part, we describe the experimental setup we have developed, associated with measurement protocols and calibration methods. Eventually, results are given for the case of single layers of dielectric materials and multilayer stacks, and we discuss the potential and limitations of the technique.

2. APPLICATION OF LIT TO OPTICAL COATINGS

A. Parametric Study

Starting with general consideration about the ability of thermography techniques to quantify the absorption level of a particular sample, it is possible as a first-order approach to evaluate the temperature increase of an absorbing sample irradiated by a laser beam. Based on the assumption of surface absorption, Gaussian beam distribution of the laser intensity, and semi-infinite medium, the temperature distribution on the surface has an expression that can be evaluated semi-analytically [27]. For continuous irradiation, the temperature in the center of the laser spot approaches the stationary value T_S:

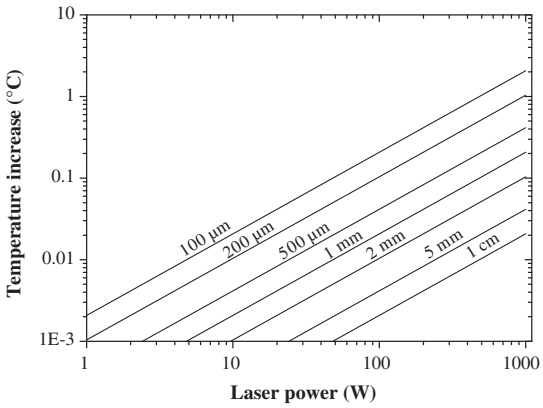

Fig. 1. Steady-state temperature increase obtained from Eq. (1) as a function of laser power for different beam diameters. $A = 1e-6$, $K = 1.36$ W/m/K.

$$T_S = \frac{AP}{2\omega K\sqrt{\pi}}, \tag{1}$$

with A the absorbed fraction of laser power P, ω the beam radius at $1/e$, and K the thermal conductivity of the material. If we consider a typical low absorptance level of 1 ppm, which corresponds to the common limit of absorption measurement methods [3], it is possible to estimate the expected temperature increase as a function of laser power and beam waist. This is done for the case of an absorbing layer on a silica substrate in Fig. 1.

The typical sensitivity of a thermal imager, or noise equivalent temperature difference (NETD), lies in the range of 25–100 mK, and can go down to 10–20 mK for the most-performing systems. In order to achieve spatially resolved absorption measurements with thermal imaging down to the ppm on a cm^2 sample, it is therefore necessary to have a kW class laser. Even if such lasers are now available, it is possible to reduce the power and scan the sample with a laser beam of few tens of watts to perform absorption mappings. In order to overcome the sensitivity limits of "passive thermography," it is possible to use active techniques such as a LIT to enhance signal-to-noise ratio: in this case, the laser power is modulated, which creates a periodic heat source with a certain lock-in frequency, and the local surface temperature modulation is evaluated and averaged over a number of periods. The main interest of lock-in techniques is that, considering their averaging nature, the effective sensitivity may improve considerably the nominal sensitivity of the sensor used. Moreover, with LIT, thermal drifts of the sensor or reflected infrared radiations from the environment are no longer disturbing the measurement. The main disadvantage of such a technique, however, is that it needs a long measurement time, since it usually averages over a number of lock-in periods. In order to evaluate the temperature increase in typical conditions of LIT measurements, the laser-induced heating process by an absorbing film was studied with finite element method (FEM), using the COMSOL software [28]. We have used for that purpose an axi-symmetric model taking into account a surface heat flux generated by absorption of laser flux with a Gaussian intensity profile at the surface of a

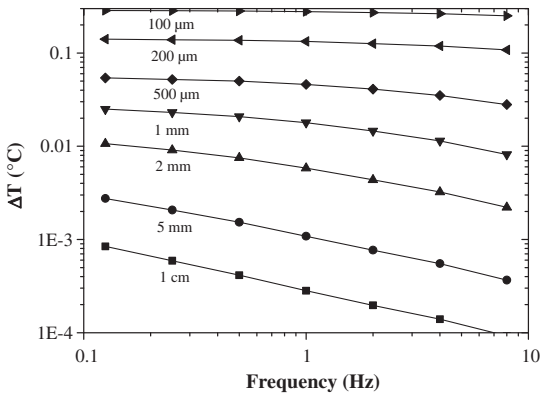

Fig. 2. Temperature modulation in the case of periodic surface heating of a silica sample, with different frequencies. Results are plotted for different beam diameters with 100 µW absorbed power.

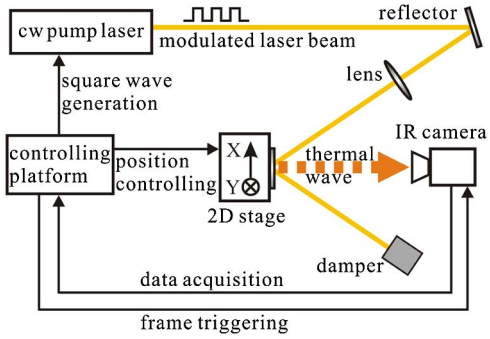

Fig. 3. Schematic of the LIT experimental setup.

silica sample (25 mm diameter and 5 mm thickness). We have simulated the temperature evolution in the case of modulated laser heating (square wave function), under assumption of heat transfers by conduction only, and extracted the modulated part of the temperature after reaching the steady state. Results are plotted in Fig. 2 in the case of 100 µW absorbed power, corresponding to the case of 100 W with 1 ppm absorption level, for different beam diameters and modulation frequencies. The modulation frequencies were kept below 10 Hz for these simulations in order to keep reasonable conditions with a classical thermal imager limited to few tens of frames per second (several frames per modulation cycle are required for LIT).

For focused beams in the range of few hundreds of micrometers, the modulated temperature, and hence expected LIT signal, is weakly dependent on the modulation frequency: the heat has time to dissipate between each pulse and the modulation depth is maximum, whatever the frequency. However, for larger beams, in the mm to cm range, the modulation depth of the temperature becomes dependent on the frequency because the beam diameter has the same order of magnitude as the characteristic length of heat diffusion. In this case, a compromise has to be found between the signal level and the measurement time. The typical conditions that were used in our work were a beam diameter of 175 µm, laser power up to 60 W, and a lock-in frequency in the range 0.25–0.5 Hz.

B. Experimental Setup and Signal Acquisition

A homemade experimental setup was built in order to apply LIT techniques to the measurement of absorption in optical coatings. An infrared Ytterbium-doped fiber laser (SPI redPOWER SP-200C) with a wavelength of 1060 nm and 200 W CW power available is used as the pump source. The laser beam is focused by a lens with 50 cm focal length and projected on the sample with a variable angle of incident (AOI), typically set to 34 deg, if not described otherwise. In such conditions, the focus spot on the sample surface has an elliptic profile of 160 by 190 µm, with a Gaussian distribution. An infrared camera (Optris PI 230) is used as the thermal sensor. It consists of an array of 160 pixels × 120 pixels microbolometers, with a pixel pitch of 25 µm, which operates in the range of 7.5–14 µm with a frame rate of 128 Hz. An IR lens with a field of view of 6° × 5° was used. The sensor was positioned at a distance of about 250 mm from the test samples; therefore, a spatial resolution of about 0.18 mm/pixel was achieved. A thermal sensitivity (NETD) of 300 mK was specified by the manufacturer. The sample was mounted on a 2D linear translation stage (Newport UTS50PP), by which a 2D mapping can be achieved. The laser illumination modulation, the camera sampling, the data acquisition and storage, and the sample movement are controlled by homemade software. A schematic of the configuration is displayed in Fig. 3.

The heat introduction can be harmonic (by sine-wave), but it is also possible to use a square-wave, i.e., a non-harmonic heat introduction. The latter one is easier for the light modulation, simple transistor–transistor logic (TTL) controlling of the laser emission, or even a mechanical chopper in the beam can work well. Meanwhile, the phase offset is more sensitive in a harmonic modulation-correlation scheme; the delay between the heating and data acquisition system should be well correlated. The non-harmonic scheme is less strict on this due to the broadband stimulation.

In the LIT technique, the raw steady-state thermographies F_j ($j = 1 - n$) are sampled by an infrared camera in one lock-in period with a fixed frame rate n (n must be even and $n \geq 4$). A discrete sine correlation function is used, as

$$K_j = 2 \sin\left(\frac{2\pi(j-1)}{n}\right), \tag{2}$$

and the in-phase lock-in photothermal signal (PS) is achieved by averaging the synchronous correlation of a series of raw thermography data $F_{i,j}$ over N lock-in periods, as

$$PS = \frac{1}{nN}\sum_{i=1}^{N}\sum_{j=1}^{n} K_j F_{i,j}. \tag{3}$$

For a complete description of the LIT technique, a quadrature signal achieved by a cosine correlation is also often taken into consideration, and a phase signal can be calculated with the in-phase and quadrature signals [14]. The phase signal is useful for detection of embedded defects but with low spatial resolution; on the other hand, the in-phase signal is proportional to the power of the thermal sources and, meanwhile, has better spatial resolution, which made it the best choice for displaying highly localized (point-like) heat sources. In this study, we focus

on the point-like thermal stimulation and measurement, so we take into consideration only of the in-phase LIT signals.

C. Measurement Protocol and Calibration Procedure

The calibration of the measurement to obtain quantitative values of absorption is not a trivial problem, since the measurement is indirect (measurement of temperature) and depends on sample properties (such as the emissivity), which are mainly unknown. We have therefore used an approach based on the use of calibration samples, as described in Ref. [5]. It relies on the assumption that the PS is linearly dependent on the absorbed power in the sample with the relationship of $A = CPS$, where C is a constant dependent on the sample properties and experimental conditions. In the case of thin films, a classical solution for the calibration is to use a sample with known absorption, then compare the signal of the sample (S) under study with the well-known absorptance of the calibration sample (CS):

$$A_{CS} = C_{CS} PS_{CS}, \tag{4}$$

$$A_S = C_S PS_S. \tag{5}$$

If the ratio $K = Cs/Ccs$ depends only on well-known experimental conditions and optical and thermal parameters, and is independent to unknown parameters, then the calibration constant K can be determined, and the absorptance of the sample can be deduced as

$$A_S = K \frac{PS_S}{PS_{CS}} A_{CS}. \tag{6}$$

To ensure the validity of such a calibration method, we have conducted numerical simulations with the FEM model described previously, and it was determined (Fig. 4) that in the test conditions, the signal depends weakly on the thermal properties or thickness of the film, but depends only on the substrate properties: if we compare two films of the same thickness but of different values of conductivity on two decades (0.3–30 W/m/K), then the error for absolute measurement of absorption is lower than 2%. Therefore, provided that the substrate of the calibration sample and the substrate of the sample under test are based on the same material, the discussed calibration method can be applied. We must emphasize that it is, however, necessary to calibrate the system for each kind of substrate used.

In this work, a series of standard absorbing samples made by ion implantation on non-absorbing material are used to calibrate the system and the measured data. They were obtained by implantation of titanium into fused-silica and BK7 substrates with different doses and have been described in Ref. [29]. The samples were 25 mm diameters with 2 mm thicknesses. Briefly, they were implanted with the following conditions: ion doses of 5×10^{16}, 2×10^{16}, 5×10^{15}, and 2×10^{15} cm^{-2} with implantation energy of 70 keV. Under these conditions, the thickness of the implanted titanium layer is approximately 100 nm [30]. Because only a thin layer is modified, it can be assumed in calculations that the thermal properties of these calibration samples are the same as the non-implanted samples (fused silica and BK7). In order to determine the optical properties and absorption of the calibration samples, the absorptance was determined by classical spectrophotometric measurements for the high-absorption samples ($A = 1 - R - T$), and the signal proportionality described in Eqs. (4) and (5) was used to determine the absorption of the samples with low implantation (Fig. 5). This is a strong assumption, but the linearity of the signal was also checked on the same samples in the experiments done with photothermal deflection a few years ago [29]. In these experiments, it was also determined that the accuracy of such a method is within the 10% range.

For the samples of interest, LIT measurement is carried out under increased pump power levels to ensure the linearity of the PS. At each pump power, four measurements at different positions on the surface of the sample (the separations are at least 1 mm) are carried out to monitor the homogeneity. For clean samples, the LIT signals are concentrated and reproducible, which means the LIT signal is dependent only on the intrinsic

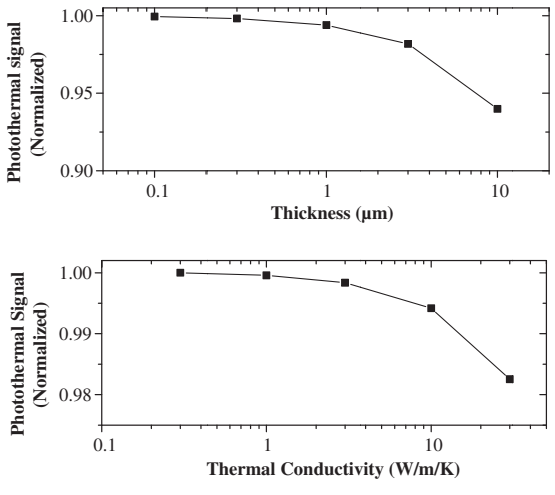

Fig. 4. Evolution of the photothermal signal in the case of a film on a fused silica substrate as a function of (a) thickness of the film and (b) thermal conductivity of the film. The simulations have been done for a frequency of 0.25 Hz and the beam size of 200 µm, as in the experiment.

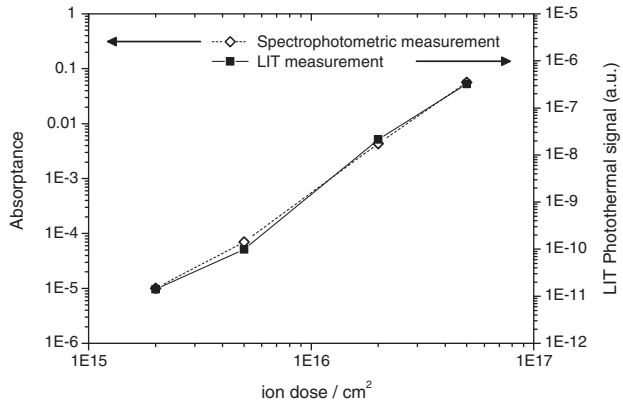

Fig. 5. Absorptance of the calibrate sample measured by classical spectrophotometric method and the photothermal signal measured by LIT method (normalized by the incident intensity), depending on the ion dose.

absorptance of the film. The mean value of the four PS signals is used to calculate the absorptance, and their standard deviation is plotted as the relative error bar.

3. RESULTS AND DISCUSSION

A. Noise Level

We have first evaluated the absorption detection limit of the experiment. For that purpose, we have measured the calibrated samples at different laser powers, staying in the linearity range, and estimated the absorption corresponding to the noise level. From these measurements, the noise equivalent absorptance was estimated as a function of the incident laser power (Fig. 6).

Based on these measurements, a limit of 1 ppm was extrapolated for our experimental conditions with a laser power of 100 W. Lower values could be achieved with the same heating power by increasing the number of periods for integrating the signal and hence reduce the noise level. This has to be compared to other measurement techniques that can achieve 1–10 ppm in most cases [5,10–12], and down to 0.1 ppm for methods with maximum sensitivity [3,31]. In our case, measurements of sample absorption of a few ppm was achieved in the experiment, as it will be shown in Section 3.

B. Measurement of Single-Layer Coatings

The absorption of single-layer Nb_2O_5 optical coating samples with different thicknesses was measured on the LIT setup. The coatings have been deposited on fused silica substrates (C7980) by plasma-assisted reactive magnetron sputtering using an HELIOS machine (Bühler). The substrates were super-polished and have been polished in the same batch (Thales-SESO). The control pressure was set to approximately 10^{-4} mbar. The film thicknesses were optically controlled during the deposition by a monochromatic transmission measurement. With the same process, samples of different optical thicknesses were manufactured and are described in Table 1.

The produced samples have been characterized by spectrophotometry with a PerkinElmer Lambda 1050. The measured reflection and transmission values were fitted by a Tauc–Lorentz model to determine refractive index. At 1060 nm, the wavelength of the laser used for LIT measurements, the determined value was $n = 2.253$.

Table 1. Properties of the Single-Layer Nb_2O_5 Coating Samples

Reference	#1	#2	#3	#4
Refractive index		2.25		
Physical thickness (nm)	30	54	61	114

LIT measurements were done on these samples in the conditions described in the previous section. The lock-in frequency was set to 0.25 Hz, one lock-in period was 4 s, and the sampling rate 8 frames per second (fps), so for each measurement point, eight periods were taken. Therefore, the measurement time was $4\ \text{s} \times 8\ \text{periods} = 32\ \text{s}$, and $8\ \text{fps} \times 32\ \text{s} = 256$ frames original data were recorded. Additionally, for each point, actually, we measured four times with increased heating power to check the linearity.

In order to analyze the data, the treatment procedure is as follows. The series of 2D thermal images are stored on the PC, then an in-phase (sinusoidal) correlation is applied with a MATLAB [32] code, and a LIT image showing the temperature-increased region is achieved. ImageJ [33] software is applied to locate the centroid of the heated region and read out the PS value. The PS values normalized by the incident intensity both for the sample of interest and the calibration sample, and the already known absorptance of the calibration sample, are used to calculate the absorptance of the sample of interest by using Eq. (6). For each measurement, four different points were measured to check the homogeneity of the sample. The mean value and the rms from these four measurements are used as the final value and the error bar, respectively.

We report in Fig. 7 on the evolution of photothermal signals achieved by the LIT method as a function of the heating power. Such measurements assess that PS-pump power relationships are in the linear region.

In the LIT measurement, the interference in the film made the light intensity through the coating dependent on the thickness. The "effective" heating power is therefore different for each film, and the electric-field distribution has to be taken into account for interpretation of LIT measurements. See, e.g., a detailed treatment of optical interference effects

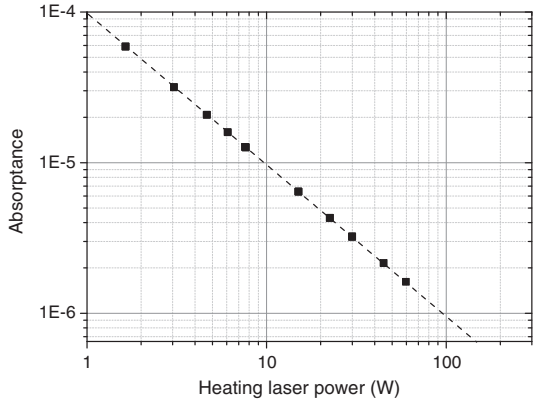

Fig. 6. Noise-equivalent absorptance with the heating laser power.

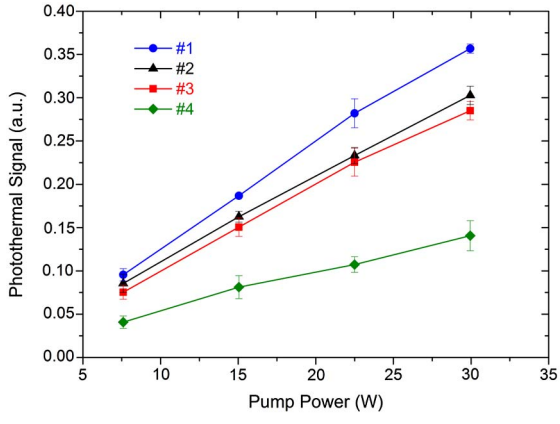

Fig. 7. Evolution of the photothermal signal achieved by LIT method with the increased heating laser power (pump power).

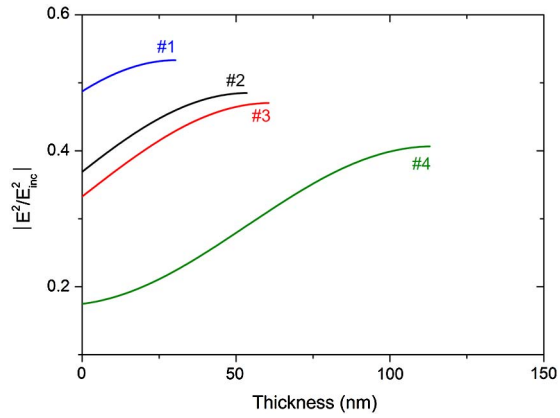

Fig. 8. Normalized electric field distributions in the Nb_2O_5 films of different thicknesses, plotted for 1060 nm wavelength.

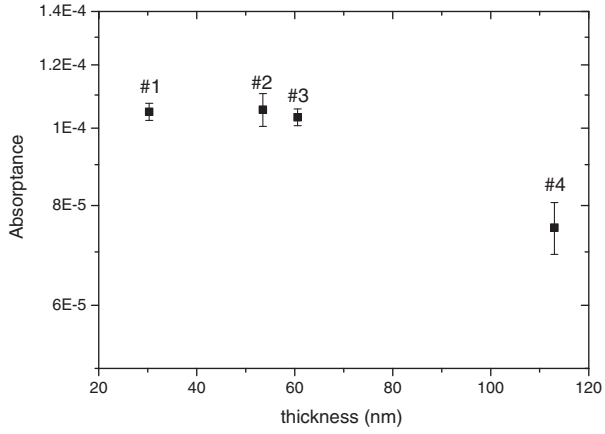

Fig. 9. Calculated absorptance for the Nb_2O_5 coatings with different thicknesses.

in photothermal measurements in multilayer coatings in Ref. [34]. These electric field distributions are calculated using the matrix method [35] for the measurement wavelength of 1060 nm, and are shown in Fig. 8.

By using the calibration procedure based on the measurement of the reference samples and taking into account the electric field distribution, the absorptance value for each sample is calculated by Eq. (6) and plotted in Fig. 9.

It can be observed that the absorptance is lowest for the sample with the thickest coating (deviation from other samples is around 20%). We do not have definitive explanations for this observation because stoechiometric or morphological analyses were not conducted on these samples. It could be related to variability in the manufacturing process or different microstructures of the films [36].

From these measurements, it was estimated an extinction coefficient of the films of $1 \pm 0.6 \times 10^{-4}$.

C. Characterization of HR Mirrors

The developed experimental technique was also applied to the characterization of optical components used in high-power laser applications (Fig. 10). We have chosen a set of commercial highly reflective mirrors from different vendors, with different optical properties: high reflectors (HR) and broadband high reflectors (BHR) for use with ultrafast lasers. The samples have, however, proprietary designs, and the structure of the multilayer stack and the materials are unknown. A summary of known samples properties is given in Table 2. Note that the samples were tested in their nominal operating conditions (angle of incidence, polarization) and that the substrates were UV fused silica for all samples.

Table 2. Properties of the Tested Mirrors[a]

Sample	*R* at 1030 nm	Bandwidth	Working AOI	Type
BHR1	>99.6%	680–1060 nm	34°	Dielectric
BHR2	>99.5%	950–1250 nm	8°	Metal/Dielectric, EBD
HR1	>99%	NA	45°	Dielectric, EBD
HR2	>99.7%	NA	45°	Dielectric
HR3	>99.5%	980–1120 nm	10°	Dielectric, EBD

[a]All mirrors were designed as high reflectors for 1.06 μm wavelength (EBD, electron beam deposition).

The measurement conditions are similar to the previous description in Section 3.B, and for the sample with lowest absorption (HR3), the laser power was set to 60 W to overcome the NETD and give a readable temperature increase.

The measurements have revealed a large dispersion in the absorptance of the samples, as shown in Fig. 10. For both broadband highly reflective mirrors, the absorptance is quite high and close to 1000 ppm. On the opposite, only a few ppm are measured for sample HR3, which is a reasonably low value compared to absorption measurements on other mirrors [12,37]. These tests illustrate the capabilities of LIT to discriminate different absorption levels on optics.

D. Absorption Mappings and Detection of Isolated Defects

Another main interest for high-power applications is the characterization of localized absorbing defects in optical components. Photothermal techniques have been widely studied to characterize absorption losses in optical components with

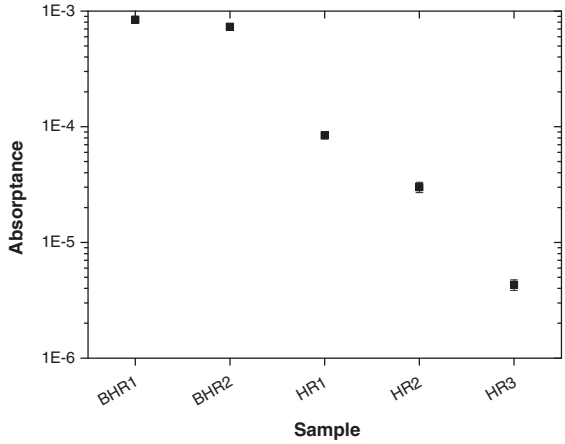

Fig. 10. Measured absorptance on the different laser mirrors.

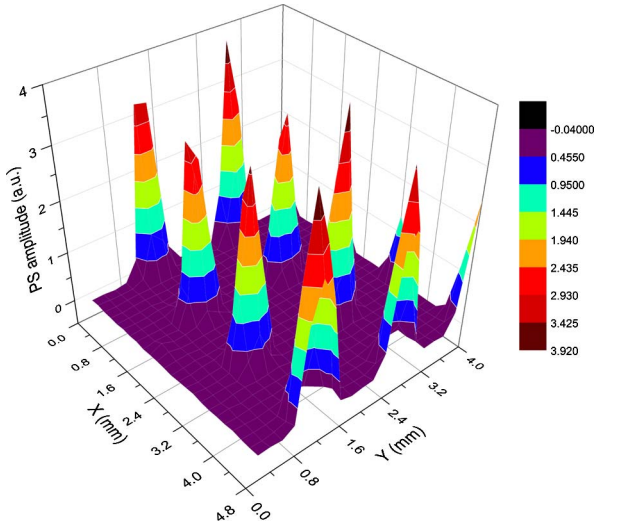

Fig. 11. 2D mapping of the absorptional photothermal signal for a metallic dot array.

high sensitivity and resolution [38–40]. In order to evaluate the potential of LIT techniques on this aspect, we have carried out an experiment with a metallic dot array (diameter ~500 μm, separation ~1.5 mm on both x and y coordinates) on glass substrate to test the ability of the technique to perform absorption mappings. By scanning the sample, the absorptance distribution can be mapped on large surfaces (compared to beam diameter) by the LIT technique. As the metallic dots are relatively absorptive, the number of lock-in period is chosen as 3, and the lock-in frequency is chosen as 0.5 Hz to speed up the test. The scanning pitch is set to 0.2 mm in both x and y directions, which is comparable to the pixel dimension at the focal plane of the IR camera. An area of 4.8 mm × 4.0 mm was scanned with the IR laser with intensity of 25.5 W/cm^2. In such conditions, a mapping velocity of approximately 100 s/mm^2 could be achieved. The mapped PS is plotted in Fig. 11. The absorbing dots, which had diameters 2.5 times the laser spot size, are well resolved with the technique, which demonstrates the ability of the technique to perform absorption mappings using stitching procedures.

However, in the case of micronic to sub-micronic isolated defects, the heated area is not resolved by the thermal imager owing to the detection wavelength in the range of 8–14 μm, which intrinsically limits the spatial resolution of IR lock-in thermography. If not resolved, an absorbing defect could still be detected if the signal received on a pixel is above the background noise. In the case, for instance, of a defect with 1 μm^2 surface cross section and considering a pixel size of 10 × 10 μm^2, 1% of the infrared energy incident on the pixel is coming from the defect contribution. However, the heating period in the LIT technique is long compared to the characteristic time for heat diffusion on a 10 μm length (<1 ms in glass), and therefore it is expected that by energy coupling from the isolated absorber to the host matrix, the heated area may be sufficient for detection of defects even with low spatial resolution. Experiments on calibrated defects (size and nature) have still, however, to be conducted to explore this possibility and are a perspective of this work.

4. CONCLUSIONS

The active LIT method was applied in the measurement of optical coatings with a homemade experimental setup in this work. The method had been verified by a set of calibration absorptive samples with standard measurement method, and the variation in results with different real sample properties had been estimated by numerical simulation. The absorptance values of different single layer coatings and multilayer stacks were evaluated in the experiment. The absorption limit of 1 ppm was reached in the experiment, and by numerical analysis, scaling of the heating laser power, increase of the number of lock-in period, and use of thermal sensor with lower NETD would still push the measurement limit forward. Compared to the traditional absorption measurement method, the LIT method shows the advantage of simpler schematic and operation, and competitive measurement ability. The 2D absorptance mapping experiment shows the potential for locating the micronic scale absorbing defects in coated optics. However, the LIT method has some drawbacks. First of all, in order to reach ppm levels or to detect micronic defects on a large surface, high-power lasers and sensitive IR cameras need to be used, and it is a relatively costly experiment. Additionally, and at least in the configuration we have used, the absorption is not directly determined, and a calibration procedure has to be implemented; also, the basic knowledge for thermal properties of the sample is needed. It should also be noted that the IR camera should operate, however, in a wavelength range where the films are not transmissive and strongly absorbing so that the emissivity is very high and only the surface temperature is measured. This was the case in our study because we have studied oxides, but it could be noted that it could be more difficult to apply the technique in the mid/far IR. Nevertheless it seems a promising technique for the field of optical components characterization.

Funding. Post-doctor scholarship grant from la Fondation Franco-Chinoise pour la Science et ses Applications (FFCSA).

Acknowledgment. Coating group of the Institut Fresnel for manufacturing and characterization of some of the samples.

REFERENCES

1. C. Jauregui, J. Limpert, and A. Tünnermann, "High-power fibre lasers," Nat. Photonics **7**, 861–867 (2013).
2. U. Willamowski, D. Ristau, and E. Welsch, "Measuring the absolute absorptance of optical laser components," Appl. Opt. **37**, 8362–8370 (1998).
3. E. Welsch and D. Ristau, "Photothermal measurements on optical thin films," Appl. Opt. **34**, 7239–7253 (1995).
4. ISO 11551: 2003(E), "Test method for absorptance of optical laser components," International Organization for Standardization, Geneva, 2003.
5. M. Commandré and P. Roche, "Characterization of optical coatings by photothermal deflection," Appl. Opt. **35**, 5021–5034 (1996).
6. Z. L. Wu, M. Reichling, X.-Q. Hu, K. Balasubramanian, and K. H. Guenther, "Absorption and thermal conductivity of oxide thin films measured by photothermal displacement and reflectance methods," Appl. Opt. **32**, 5660–5665 (1993).

7. H. Hao, A. Zhou, and M. Rao, "Study on the absorption uniformity of optical thin films based on the photothermal detuning technique," Appl. Opt. **51**, 6844–6847 (2012).
8. J. P. Bourgoin, G. G. Allogho, and A. Haché, "Thermal conduction in thin films measured by optical surface thermal lensing," J. Appl. Phys. **108**, 073520 (2010).
9. W. J. Choi, S. Y. Ryu, J. K. Kim, J. Y. Kim, D. U. Kim, and K. S. Chang, "Fast mapping of absorbing defects in optical materials by full-field photothermal reflectance microscopy," Opt. Lett. **38**, 4907–4910 (2013).
10. C. Mühlig, S. Kufert, S. Bublitz, and U. Speck, "Laser induced deflection technique for absolute thin film absorption measurement: optimized concepts and experimental results," Appl. Opt. **50**, C449–C456 (2011).
11. B. Li, D. Ristau, and H. Blaschke, "Combined laser calorimetry and photothermal technique for absorption measurement of optical coatings," Appl. Opt. **45**, 5827–5831 (2006).
12. J. Steinlechner, L. Jessica, C. Krüger, N. Lastzka, S. Steinlechner, and R. Schnabel, "Photothermal self-phase-modulation technique for absorption measurements on high-reflective coatings," Appl. Opt. **51**, 1156–1161 (2012).
13. G. Busse, D. Wu, and W. Karpen, "Thermal wave imaging with phase sensitive modulated thermography," J. Appl. Phys. **71**, 3962–3965 (1992).
14. O. Breitenstein, W. Warta, and M. Langenkamp, *Lock-in Thermography, Basics and Use for Evaluating Electronic Devices and Materials* (Springer, 2010).
15. X. P. V. Maldague, *Theory and Practice of Infrared Technology for Nondestructive Testing* (Wiley, 2001).
16. M. Choi, K. Kang, J. Park, W. Kim, and K. Kim, "Quantitative determination of a subsurface defect of reference specimen by lock-in infrared thermography," NDT&E Int. **41**, 119–124 (2008).
17. H. Song, H. J. Lim, S. Lee, H. Sohn, W. Yun, and E. Song, "Automated detection and quantification of hidden voids in triplex bonding layers using active lock-in thermography," NDT&E Int. **74**, 94–105 (2015).
18. A. Semerok, F. Jaubert, S. V. Fomichev, P.-Y. Thro, X. Courtois, and C. Grisolia, "Laser lock-in thermography for thermal contact characterisation of surface layer," Nucl. Instrum. Methods Phys. Res. A **693**, 98–103 (2012).
19. P. D. Allen, B. Nadal-Ginard, and R. M. Medford, "Using lock-in infrared thermography for the visualization of the hand vascular tree," Proc. SPIE **6939**, 69390O (2008).
20. D. Wu, H. Hamann, A. Salerno, and G. Busse, "Lock-in thermography for imaging of modulated flow in blood vessels," in *Quantitative Infrared Thermography 3 (QIRT'96)* (Edizioni ETS, 1997), p. 343.
21. O. Breitenstein, M. Langenkamp, F. Altmann, D. Katzer, A. Lindner, and H. Eggers, "Microscopic lock-in thermography investigation of leakage sites in integrated circuits," Rev. Sci. Instrum. **71**, 4155–4160 (2000).
22. M. Bail, J. Kentsch, R. Brendel, and M. Schulz, "Lifetime mapping of Si wafers by an infrared camera," in *28th IEEE Photovoltaic Specialists Conference* (2000), p. 99.
23. S. Riepe, J. Isenberg, C. Ballif, S. W. Glunz, and W. Warta, "Carrier density and lifetime imaging of silicon wafers by infrared lock-in thermography," in *17th European Photovoltaic Solar Energy Conference* (2001), p. 1597.
24. O. Breitenstein, J. P. Rakotoniaina, M. H. Al Rifai, and M. Werner, "Shunt types in crystalline silicon solar cells," Prog. Photovoltaics **12**, 529–538 (2004).
25. M. Kaes, S. Seren, T. Pernau, and G. Hahn, "Light-modulated lock-in thermography for photosensitive *pn*-structures and solar cells," Prog. Photovoltaics **12**, 355–363 (2004).
26. J. Isenberg and W. Warta, "Realistic evaluation of power losses in solar cells by using thermographic methods," J. Appl. Phys. **95**, 5200–5209 (2004).
27. M. D. Feit and A. M. Rubenchik, "Mechanisms of CO_2 laser mitigation of laser damage growth in fused silica," Proc. SPIE **4932**, 91 (2003).
28. https://www.comsol.com/comsol-multiphysics.
29. L. Gallais and M. Commandré, "Simultaneous absorption, scattering, and luminescence mappings for the characterization of optical coatings and surfaces," Appl. Opt. **45**, 1416–1424 (2006).
30. S. Tisserand, F. Flory, A. Gatto, L. Roux, M. Adamik, and I. Kovacs, "Titanium implantation in bulk and thin film amorphous silica," J. Appl. Phys. **83**, 5150–5153 (1998).
31. A. C. Boccara, D. Fournier, W. Jackson, and N. M. Amer, "Sensitive photothermal deflection technique for measuring absorption in optically thin media," Opt. Lett. **5**, 377–379 (1980).
32. https://www.mathworks.com/products/matlab.html.
33. https://imagej.nih.gov/ij/.
34. L. Gallais and M. Commandré, "Photothermal deflection in multilayer coatings: modeling and experiment," Appl. Opt. **44**, 5230–5238 (2005).
35. H. A. Macleod, *Thin-Film Optical Filters* (IOP, 2001).
36. T. J. Bright, J. I. Watjen, Z. M. Zhang, C. Muratore, and A. A. Voevodin, "Optical properties of HfO_2 thin films deposited by magnetron sputtering: from the visible to the far infrared," Thin Solid Films **520**, 6793–6802 (2012).
37. C. Mühlig, W. Triebel, S. Kufert, and S. Bublitz, "Characterization of low losses in optical thin films and materials," Appl. Opt. **47**, C135–C142 (2008).
38. M. Selmke, M. Braun, and F. Cichos, "Photothermal single-particle microscopy: detection of a nanolens," ACS Nano **6**, 2741–2749 (2012).
39. M. Selmke, A. Heber, M. Braun, and F. Cichos, "Photothermal single particle microscopy using a single laser beam," Appl. Phys. Lett. **105**, 013511 (2014).
40. A. During, M. Commandré, C. Fossati, B. Bertussi, J. Natoli, J. Rullier, H. Bercegol, and P. Bouchut, "Integrated photothermal microscope and laser damage test facility for in-situ investigation of nanodefect induced damage," Opt. Express **11**, 2497–2501 (2003).